An Attempt to Simulate the Bowing Phenomenon in Tenter with Simple Models

TOSHIRO YAMADA* and CHISATO NONOMURA

Toyobo Co., Ltd., Toyobo Research Institute, 1-1 Katata 2-chome, Ohtsu, Shiga, 520-02 Japan

SYNOPSIS

The bowing phenomenon throughout a tenter was experimentally observed with a pilot plant of successive biaxial stretching. The observed results were compared with simulated ones, by which the deformation behaviors of film in a tenter were predicted, with the assumption that the film was homogeneous isotropic, homogeneous anisotropic, heterogeneous isotropic, or heterogeneous anisotropic for a two-dimensional elastic body with an FEM. Comparatively good agreement between the simulated and observed results was obtained for a heterogeneous anisotropic elastic body with an initial mesh, involving in advance a plastic deformation part. © 1993 John Wiley & Sons, Inc.

INTRODUCTION

It is a common practice to stretch a film made of linear thermoplastic polymer, such as polypropylene, poly(ethylene terephthalate), polyethylene, nylon, or polystyrene, in order to produce an orientation that will upgrade the film's performances. The polymer films are used for various purposes and therefore, their higher qualities have been required year by year. The demand for the more useful qualities of the film brings about the demand for better techniques of film processing, especially in the area of the stretching techniques for films, by which the superior characteristics of films become evident. The stretching methods are classified roughly into flat film stretching and tubular inflation. In stretching a flat film in the transverse direction, a tenter is usually used.

Many articles describe the properties of the mono- or bioriented stretched films, however, articles discussing the technology of the industrial stretching of films are small in number. Especially few papers are available on the film deformation behavior in the tenter process and the tenter has usually been dealt with as a "black box" that defies analysis because of its high cost and the complexity of the film behavior in it.

The representative and common problems in the stretching of polymer films are the "bowing" phenomenon, which causes the nonuniformity of film characteristics in the transverse direction, the "necking" phenomenon, which causes the decrease in the available width of film, and the thickness unevenness of film, which causes the planar waviness of film and the wrinkle in the winding of film.

The bowing phenomenon, for example, is one of the most serious problems in the tenter process. The bowing phenomenon causes the descrepancy between the direction of the orientation axis at the center of film width and the direction at the edges, and the anisotropy of film characteristics, such as the heat shrinkage, the refractive index, and mechanical properties. For example, the bowing phenomenon causes a lowering of magnetic recording characteristics of the base film for floppy disc use, requiring the isotropy in a plane of film properties, an aberration of printing in the printing and laminating processes, and a curl in the bagging process for a package use.

Articles on the bowing phenomenon have been published by Kase et al.[1-4] and Sakamoto.[5,6] Kase et al. have theoretically analyzed the deformation behavior of thin, uneven rubber film in the tenter process with the finite difference method (FDM). Sakamoto has reported on the theoretical analysis of an ellipsoidal refractive index as an optical anisotropy of poly(ethylene terephthalate) (PET) film,

* To whom correspondence should be addressed.

Journal of Applied Polymer Science, Vol. 48, 1399–1408 (1993)
 CCC 0021-8995/93/081399-10

due to the bowing phenomenon. These predicted results have not confirmed experimentally, however, with the tenter process.

In this article, the observations of the bowing phenomenon throughout the tenter process with a pilot plant and their theoretical analysis by a finite element method (FEM) with simple models are reported.

DEFINITION OF BOWING DISTORTION

The bowing phenomenon is a characteristic problem, occurring in the stretching and thermosetting of film in a tenter process. Various film manufacturing methods, using a tenter, now exist and various mechanisms to produce the bowing phenomenon occur, depending upon the method. Thus, the stretching method in this article is described.

Manufacturing Method of Biaxially Oriented Film

The manufacturing method of biaxially oriented film with a tenter is roughly divided into two parts. One is a successive stretching method, which is divided into the longitudinal machine direction (MD) stretching–transverse (TD) stretching method and the TD–MD method. Another part of the method is a simultaneous stretching method in both MD and TD. In this article, the successive MD–TD method, shown in Figure 1, was used. The MD–TD method is superior to other methods in productivity, which is a typical tenter process for the successive biaxial stretching of PET films. In Figure 1, the extruder (EXT) melts and extrudes the polymer. The extruded film is cast (CA) on a chill roll in order to form an amorphous sheet. The PET sheet is subsequently stretched in the machine direction (MD) to become the mono-oriented film. The film is then stretched in the transverse direction (TD) and thermoset (TS) to become the bioriented film. The film is finally trimmed (TM) and taken up on the film winder (FW).

In the (TD) and (TS) sections of the tenter process, films often develop the bowing phenomenon. Bowing is a kind of uneven stretching, in which a straight line, drawn transversely on the film entering the tenter, bends in a bow shape as the film goes through the (TD) and (TS) sections.

Definition of Bowing Distortion

In the manufacture of a biaxially oriented film with a tenter, the bowing phenomenon is inevitable. The bowing phenomenon is divided into two parts. One is a geometrical bowing phenomenon, in which a straight line drawn across the width of the film at the entrance of a tenter changes into a bow shape at the exit of the tenter. Another part is a characteristic bowing phenomenon, in which the state of molecular orientation is different at each point across the width of film and, as a result, the characteristics of the film are ununiform over the film width. In this article, the geometrical bowing phenomenon is dealt with under the assumption that the geometrical bowing phenomenon corresponds to the characteristic bowing phenomenon.

As shown in Figure 2, the distortion of bowing is expressed as the bow height, b, which is presented as a percentage of the film width, W. When the film center lags behind the film edges, the bow height b is considered positive. The bowing distortion b/W, measured at different positions within the (TD, TS) sections, consists of four zones: preheating, stretching in the transverse direction, thermosetting, and cooling, as indicated in Figure 2.

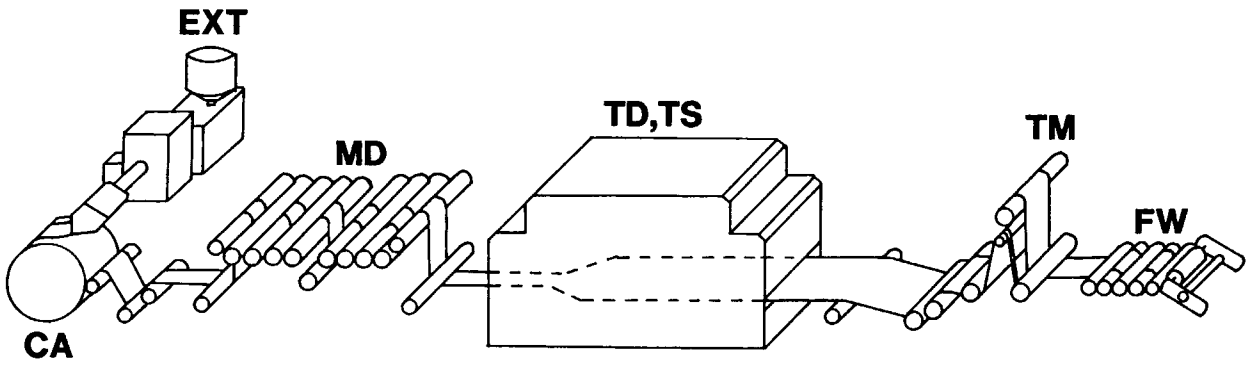

Figure 1 Schematic of representative film production process.

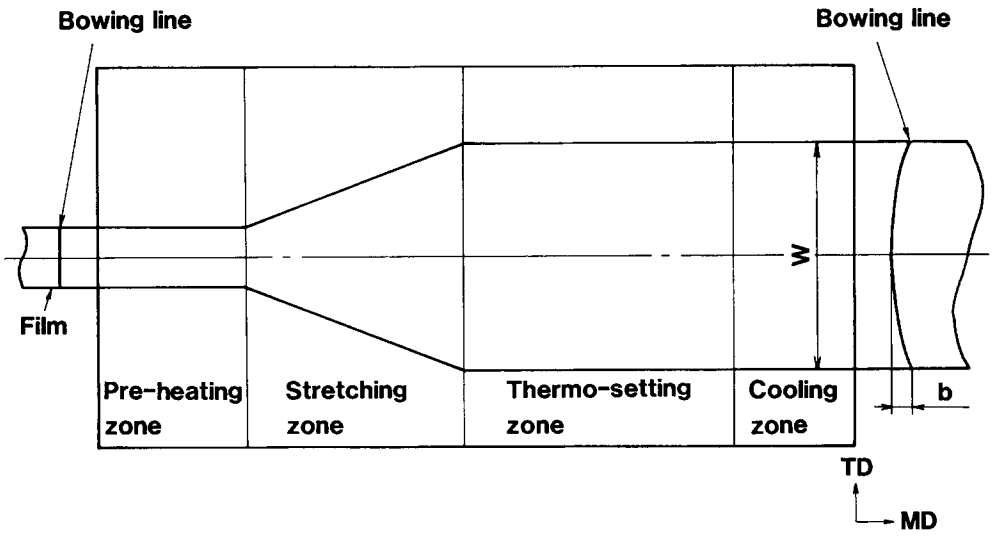

Figure 2 Four zones of tenter.

EXPERIMENTAL

The experiments[7] were made using a pilot plant, as shown in Figure 1.

The PET polymer was melted and extruded on a chill roll and was then formed into an amorphous film shape. After applying different rotational speeds of rollers, the as-cast amorphous film was drawn longitudinally (in the machine direction), with infrared heaters at the drawing ratio of 3.5 magnification. The preheating roller temperature was 60°C, the drawing roller temperature was 90°C, and the cooling roller temperature was 40°C.

The uniaxially oriented PET film was transversely stretched by the tenter, while being held by the tenter clips, at the extention ratio of 3.6 magnification. The film was then formed into biaxially oriented film. As shown in Figure 2, the tenter was divided into four zones, consisting of the preheating, transverse stretching, thermosetting, and cooling zones. The temperature of each zone was set at 90°C in the preheating zone, 100°C in the transverse stretching zone, 150°C to 225°C in the thermosetting zone, and 75°C to 200°C in the cooling zone, respectively, as shown in Table I. The transverse relaxation ratio was −10 to 20%, as shown in Figure 3, where a negative value denotes the transverse restretching and a positive value denotes the transverse relaxation.

RESULTS AND DISCUSSION

Observation of Bowing Distortion Throughout the Tenter Process

Many straight lines across the width of the film were drawn on the surface of the film at the entrance of the tenter. After forcing the movement of the tenter chains to stop, and the film in the tenter to cool as soon as possible by electric fans, the whole film in the tenter, shaped into the rectangular–ramp–rectangular tenter form, as shown in Figure 2, was sampled. It was confirmed that the bowing distortions hardly changed during the cooling of film. The

Table I Experimental Conditions

Stretching Ratio in TD (−)	Preheating Temperature (°C)	Stretching Temperature (°C)	Thermosetting Temperature (°C)	Cooling Temperature (°C)	Relaxation Ratio in TD (%)
3.6	90	100	150	75	−10
			175	100	0
			200	150	10
			225	200	20

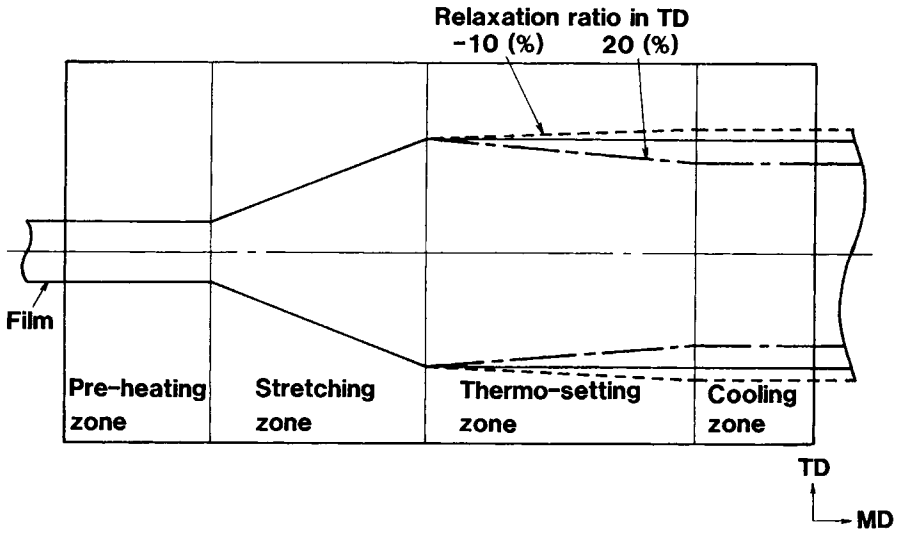

Figure 3 TD relaxation patterns in the thermosetting zone.

lines were marked by a comparison of the distortions near the exit of tenter before cooling with those after cooling.

Using the film obtained by the above procedures, the changes in the bowing distortions throughout the whole tenter were measured. Shown in Figure 4 are the changes in the distortion b/W of experimentally-observed bowing, as the film goes through the (TD, TS) sections. In Figure 4, the position in the tenter is expressed as the dimensionless length L/W, which is the distance from the entrance of the tenter, L, divided by the film width, W. In Figure 4 it is noted that bowing remains insignificant in the preheating zone. As the film enters the transverse stretching zone, the film develops a negative bowing, followed by a quick change into positive bowing. Bowing takes its maximum positive value in the first half of the thermosetting zone. Thereafter, the bowing maintains a high positive level.

The bowing phenomenon can be considered to occur as follows: Both edges of film, held by the chain clips of the tenter, are bound, whereas the binding force due to the chain clips decreases approaching the center of film width. As a result, the longitudinal (machine direction) force, generated by the transverse stretching and the heat shrinkage in the tenter, causes the bowing phenomenon. Since the stiffness of film in the thermosetting zone is lowest, due to

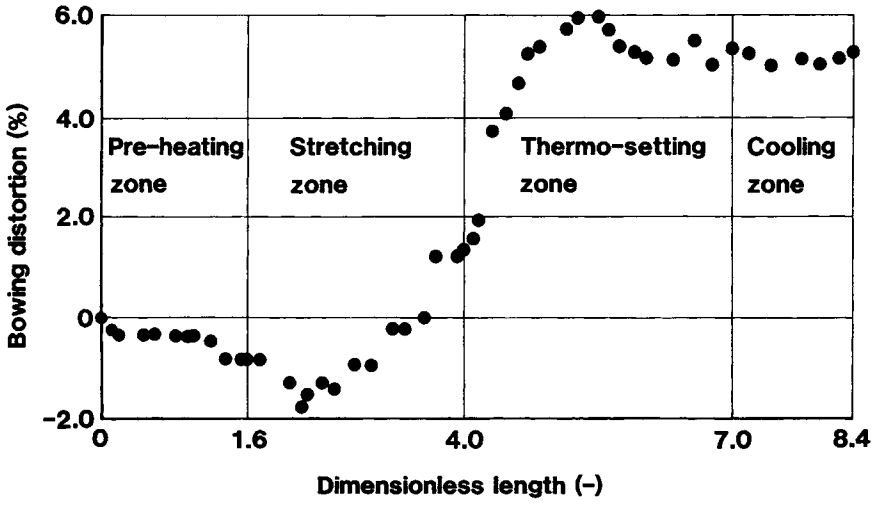

Figure 4 Experimentally observed deformation behavior in tenter, expressed in bowing distortion vs. dimensionless length.

the highest temperature in the tenter, the longitudinal force greatly affects and enlarges the bowing distortion in the thermosetting zone.

The bowing distortion in the thermosetting zone has a maximum value near the beginning of the thermosetting zone and subsequently remains constant at the maximum value. The temperature of film reaches the highest value near the beginning of the thermosetting zone. As a result, the film has the lowest stiffness and the highest heat shrinkage near the beginning of thermosetting zone. Therefore, the film is deformed by the longitudinal force, due to the heat shrinkage and the transverse stretching at the highest temperature position, which produces a maximum bowing distortion. Thereafter the film remains at maximum bowing distortion under the highest temperature or less because the longitudinal force does not occur again.

The above results are different than the assumptions for the theory of Sakamoto,[5,6] who suggests that the bowing distortions have only positive values and become gradually larger in the machine direction.

Effect of Thermosetting Temperature on Bowing Distortion

Figure 5 shows the effect of the thermosetting temperatures on the bowing distortion under the conditions of the preheating temperature of 90°C, the transverse stretching temperature of 100°C, the cooling temperature of 100°C, and the transverse relaxation ratio of 0% (no transverse relaxation) in the tenter. Figure 5 shows that higher thermosetting temperatures tend to increase the distortion of bowing because a higher thermosetting temperature yields a lower stiffness and a higher heat shrinkage of film.

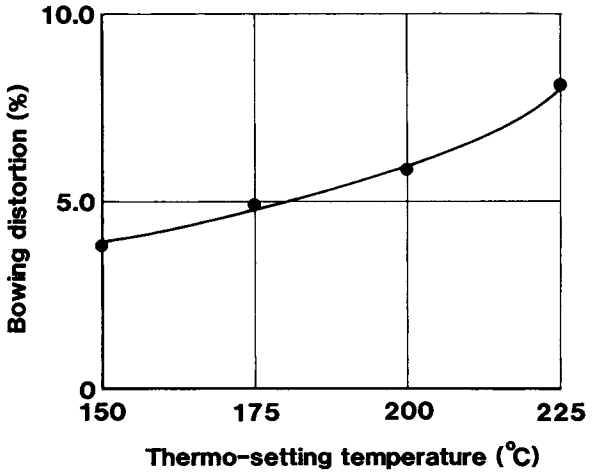

Figure 5 Bowing distortion at tenter exit vs. thermosetting temperature.

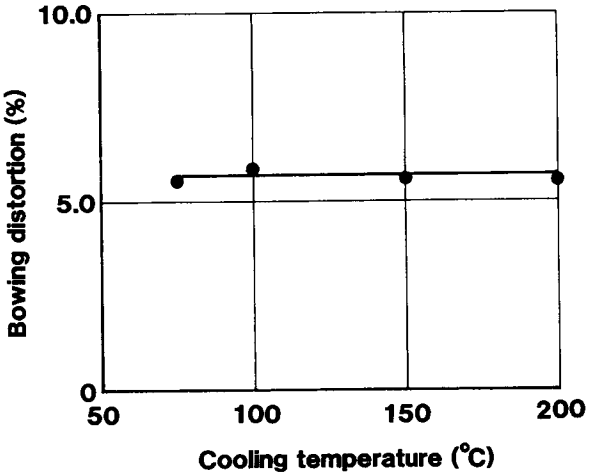

Figure 6 Bowing distortion at tenter exit vs. cooling temperature.

Effect of Cooling Temperature on Bowing Distortion

Figure 6 shows the effect of the cooling temperatures on the bowing distortion under the conditions of the preheating temperature of 90°C, the transverse stretching temperature of 100°C, the thermosetting temperature of 200°C, and no transverse relaxation in the tenter. As shown in Figure 6, changing the temperature of cooling does not affect the bowing distortion. This may be the reason that the heat shrinkage of film hardly occurs in the cooling zone and the stiffness of film in the cooling zone is higher than that in the thermosetting zone since a cooling temperature is lower than a thermosetting one.

Effect of Transverse Relaxation on Bowing Distortion

Figure 7 shows the effect of the transverse relaxations on the bowing distortion under the conditions of the preheating temperature of 90°C, the stretching temperature of 100°C, the thermosetting temperature of 200°C, and the cooling temperature of 100°C in the tenter. It was found that allowing the film to shrink transversely in the thermosetting zone, that is, relaxing, tended to increase bowing, as shown in Figure 7. Negative relaxing, that is, restretching, in the thermosetting zone tended to surpresses bowing. This may be the reason that the binding force, due to the chain clips, becomes weaker

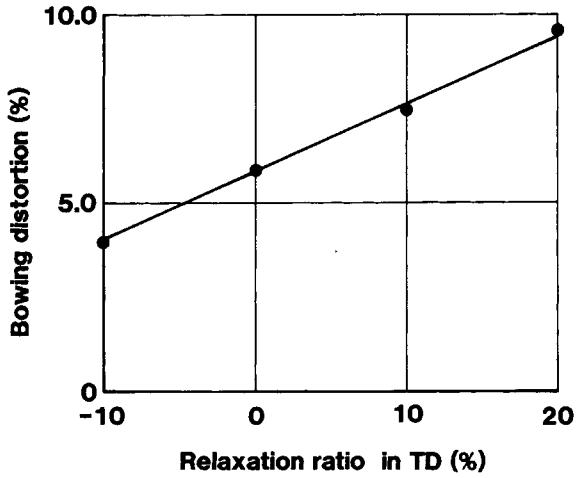

Figure 7 Bowing distortion at tenter exit vs. relaxation ratio in TD within thermosetting zone.

and the film becames easy to be deformed at the higher transverse relaxation ratio.

Simulation of Bowing Phenomenon in the Tenter Process

A FEM simulation of the bowing phenomenon, occurring in the (TD, TS) sections of the tenter process, was carried out, assuming the film to be a thin (two dimensional) elastic body.

As tabulated in Table II, four different materials were considered: homogeneous isotropic, homogeneous anisotropic, heterogeneous isotropic, or heterogeneous anisotropic. The shape of the film before stretching was assumed to be a rectangle (initial shape a) or a rectangle-plus-ramp shape (initial shape b), as shown in Figure 8. The width of the initial rectangle was considered to be equal to the width of the film entering the (TD) section of the tenter. Initial division of the film shape into triangular elements is shown in Figure 8.

The film shapes in Figure 8 are intended to cover the region extending from the entrance of the tenter to the point of maximum temperature, located in the thermosetting zone. This choice was made because, throughout the region between the maximum temperature point and the tenter exit, the extent of bowing was known experimentally to remain unchanged.

Figures 9 to 13 compare experimental observations of b/W values with the results of the FEM simulation. Bowing is considered to be positive when the bow shape is concave toward tenter exit, that is, when the film center lags behind the film edges.

For an anisotropic material, four independent elastic constants exist, E_x, E_y, G_{xy}, and ν_{xy}. In these constants, the G_{xy} is given by the following equation:

$$\frac{1}{G_{xy}} = \frac{4}{E_{45}} - \left(\frac{1}{E_x} + \frac{1}{E_y} - \frac{2\nu_{xy}}{E_x}\right) \tag{1}$$

where E_x and E_y are the Young's moduli, G_{xy} is the

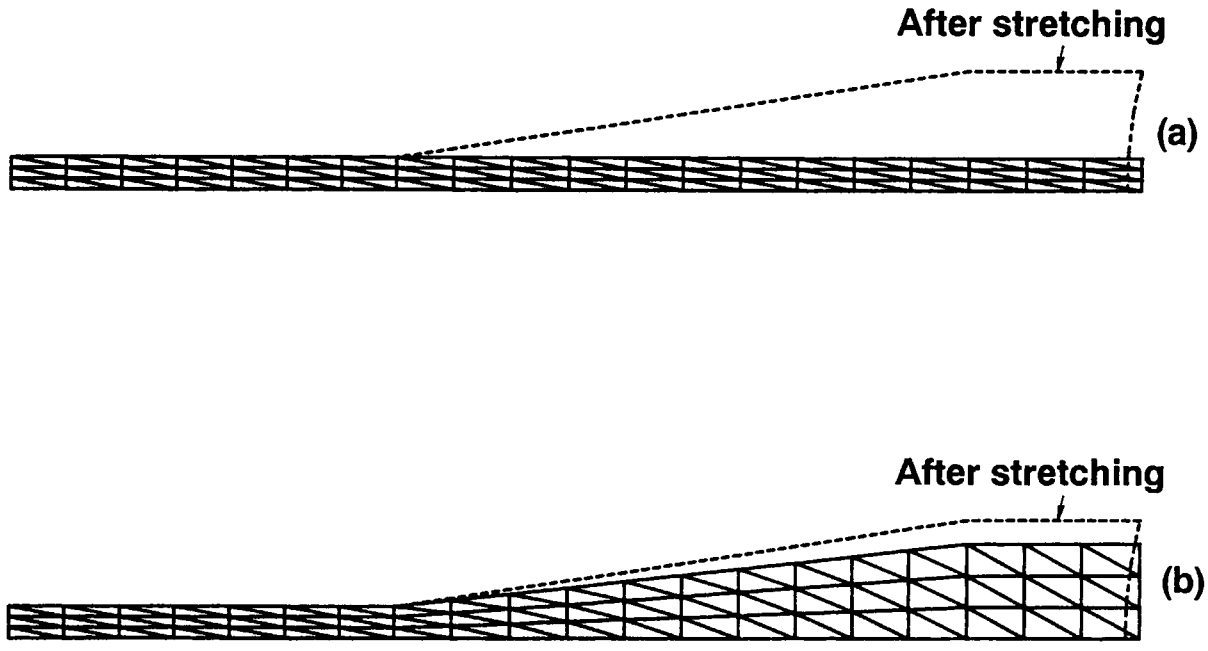

Figure 8 Two kinds of initial mesh.

shear modulus (rigidity), ν_{xy} is the Poisson's ratio, and E_{45} is the Young's modulus in a direction at an angle of 45° to the machine (longitudinal) direction, which is derived from the average of E_x and E_y; $E_{45} = (E_x + E_y)/2$ and the subscripts x and y stand for longitudinal (machine) direction and transverse direction, respectively. In addition to the above, the Maxwell–Betti reciprocal theorem states that $\nu_{yx}/\nu_{xy} = E_y/E_x$. Isotropic materials were assumed to have two independent elastic constants E and ν, meaning that $E = E_x = E_y = E_{45}$ and $\nu = \nu_{xy} = \nu_{yx}$.

In the FEM computations, fixed values were given to the above elastic constants at the entrance and exit of each zone and the values within the zone were assumed to be linear interpolations of values at the entrance and exit.

Figure 9 compares the experimental results with the FEM simulation, assuming the film to be homogeneous isotropic and to have the initial shape *a* (rectangle). The simulation is not satisfactory.

Figure 10 is the same as Figure 9, except that in the FEM simulation, the film material was assumed to be a homogeneous anisotropic that had four independent elastic constants E_x, E_y, G_{xy}, and ν_{xy}.

Figure 10 shows a comparison of the experimental results with the calculated results under the assumption that the film is a homogeneous anisotropic material with the initial film shape of a rectangle, as shown in Figure 8(a). Evidently, the simulation shown in Figure 10 is not good enough.

Figure 11 shows the comparison for the case of heterogeneous isotropic film *a* (rectangle) in the initial shape. Again, the simulation is not entirely satisfactory.

Figure 12 shows the case of the heterogeneous anisotropic film *a* (rectangle) in initial shape. The FEM simulation in this case is worse than the one in Figure 11.

Figure 13 shows the case of the heterogeneous anisotropic film *b* [rectangle-plus-ramp, see Fig. 8(b)] in initial shape. This particular initial film shape *b* was conceived to take into consideration about 20% shrinkage of the bioriented film, entering the thermosetting zone at 105°C, and approaching the transverse stretching temperature. In other words, the ramp part of the initial film shape was intended to include in advance the plastic deformation, measured as the shrinkage of the film just after the transverse extension. The simulation, shown in Figure 13 is more satisfactory than any of these shown in Figures 9 to 12. Agreement with experimental values is particularly good at and after the point at which the bowing turns from negative to positive values.

Table II Simulation Conditions

Case No.	Mesh Type	Material Constants															
		Preheating Zone						Stretching Zone						Thermosetting Zone			
		Start			End			Start			End			Start			End		
		E_x (GPa)	E_y (GPa)	ν_{xy} (—)	E_x (GPa)	E_y (GPa)	ν_{xy} (—)	E_x (GPa)	E_y (GPa)	ν_{xy} (—)	E_x (GPa)	E_y (GPa)	ν_{xy} (—)	E_x (GPa)	E_y (GPa)	ν_{xy} (—)	E_x (GPa)	E_y (GPa)	ν_{xy} (—)
1	*a*	4.000	4.000	0.36	4.000	4.000	0.36	4.000	4.000	0.36	4.000	4.000	0.36	4.000	4.000	0.36	4.000	4.000	0.36
2	*a*	4.000	1.000	0.36	4.000	1.000	0.36	4.000	1.000	0.36	4.000	1.000	0.36	4.000	1.000	0.36	4.000	1.000	0.36
3	*a*	4.500	4.500	0.36	4.500	4.500	0.34	4.000	4.000	0.36	4.000	4.000	0.36	0.500	0.500	0.42	0.500	0.500	0.42
4	*a*	4.500	1.125	0.34	4.500	1.125	0.34	4.000	1.000	0.36	4.000	4.000	0.36	0.500	0.500	0.42	0.500	0.500	0.42
5	*b*	4.500	1.125	0.34	4.500	1.125	0.34	4.000	1.000	0.36	4.000	4.000	0.36	4.000	4.000	0.36	0.500	0.500	0.42

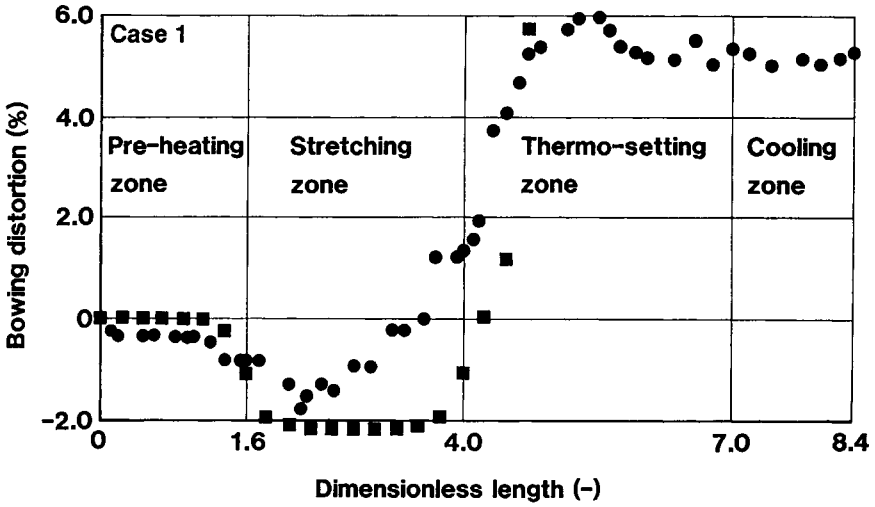

Figure 9 Bowing, experiment and FEM simulation, Case 1 in Table II. (●) Experimental, (■) Calculated.

A summary of the results observed and simulated is shown below.

The successive distortion patterns of the drawn lines were observed over the whole tenter in order to analyze the bowing phenomenon, which causes unevenness of the film properties over the width of the film. From observation, the following results were obtained:

1. A straight line, drawn across the width of film before the preheating zone, does not change during the preheating zone and remains straight. In the beginning region of the transverse stretching zone, the line changes into a convex curve (reverse bowing) in the travelling direction of film and the convex distortion becomes maximum in the zone. Near the end of the zone, the line becomes again straight and at the end of the zone the line changes into a concave curve. Near the beginning of the thermosetting zone, the concave distortion reaches maximum; after this, the line does not change and it remains at the maximum concave distortion (bowing distortion), which is usually observed as a bowing phenomenon.
2. A higher temperature of thermosetting produces more bowing distortion.
3. The temperature of cooling does not influence the bowing distortion.

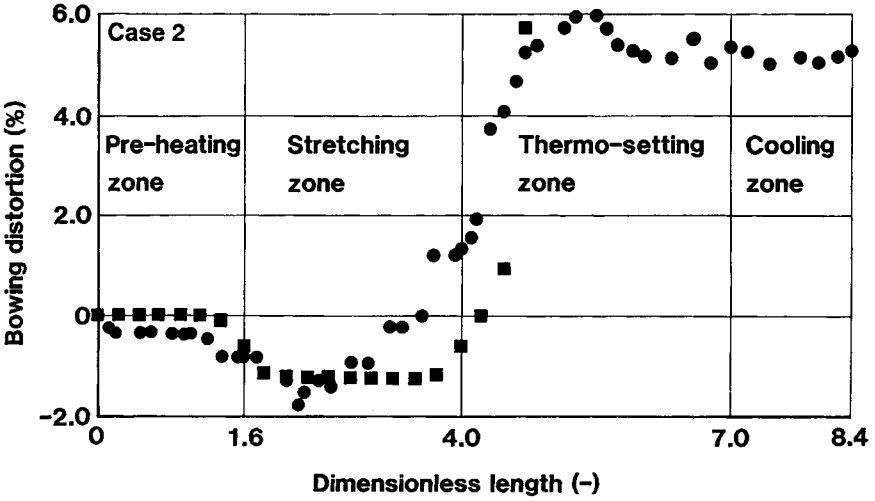

Figure 10 Bowing, experiment and FEM simulation, Case 2 in Table II. (●) Experimental, (■) Calculated.

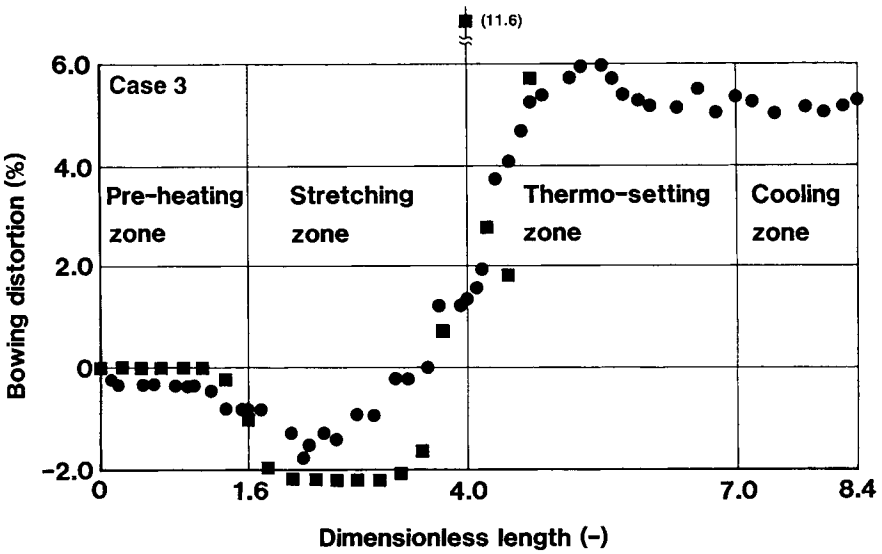

Figure 11 Bowing, experiment and FEM simulation, Case 3 in Table II. (●) Experimental, (■) Calculated.

4. The relaxation, or restretching, in the transverse direction in the thermosetting zone influences the bowing distortion; a higher relaxation produces more bowing distortion and higher restretching yields less bowing distortion.
5. A heterogeneous anisotropic model, with the initial mesh including the plastic deformation in advance, can express comparatively well the bowing distortion pattern of film throughout a tenter by an FEM simulation. The above results suggest that an elastic-plastic body is effective for the simulation of the bowing phenomenon with an FEM.

CONCLUSIONS

The bowing phenomenon was first observed throughout the tenter process. It was confirmed that the bowing distortion changes from a convex curve (reverse bowing) to a concave curve (bowing) in the travelling direction of film.

The simulation by an FEM was attempted for

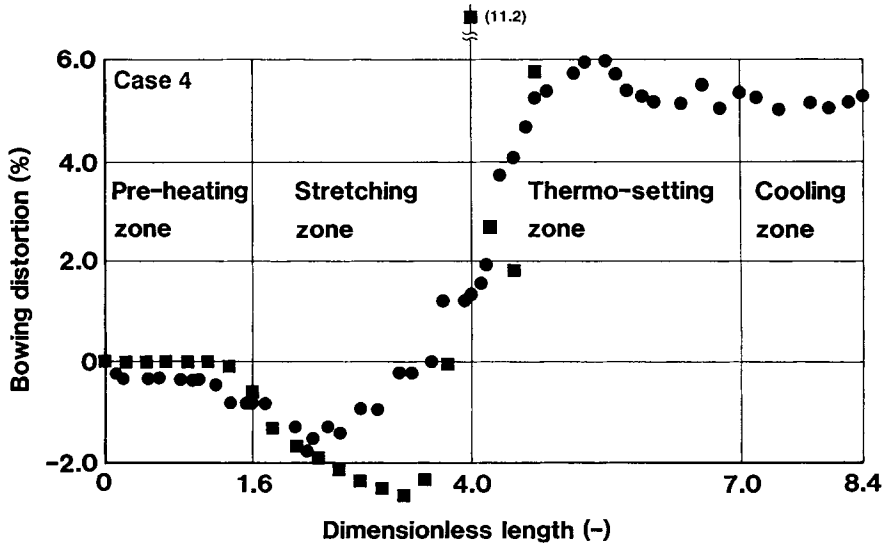

Figure 12 Bowing, experiment and FEM simulation, Case 4 in Table II. (●) Experimental, (■) Calculated.

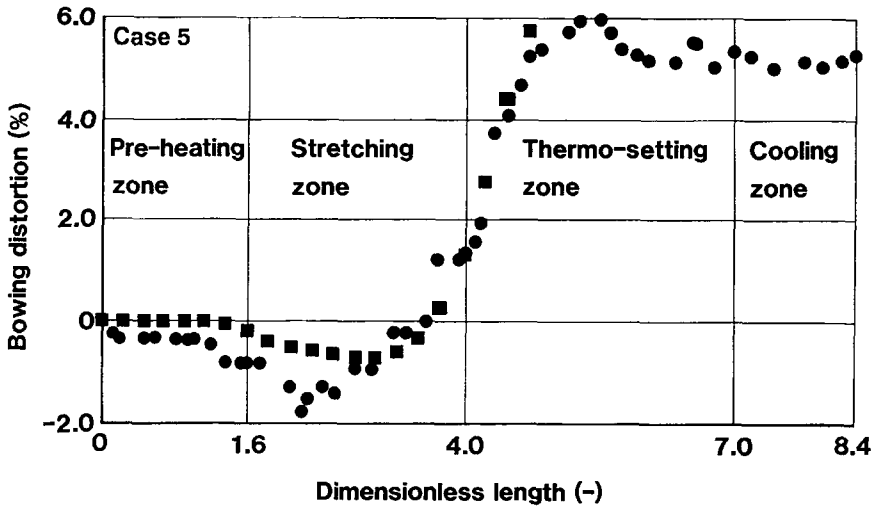

Figure 13 Bowing, experiment and FEM simulation, Case 5 in Table II. (●) Experimental, (■) Calculated.

the deformation behavior of film in a tenter with simple models, under the assumption that the film was a two-dimensional elastic body. Simulated results for assuming the film to be an heterogeneous anisotropic, which had a rectangle-plus-ramp initial shape, agreed approximately with the observed results.

The authors thank Toyobo Co., Ltd., for permission to publish this work.

REFERENCES

1. S. Kase, T. Nishimura, Y. Sonoda, M. Kado, and K. Takuma, *Bulletin of the Faculty of Textile Science,* Kyoto Institute of Technology, **12,** 33–50 (1988).
2. T. Nishimura, S. Kase, and K. Hino, *Bulletin of the Faculty of Textile Science,* Kyoto Institute of Technology, **13,** 69–80 (1989).
3. S. Kase and T. Nishimura, *J. Rheol.,* **34,** 251–273 (1990).
4. S. Kase, N. Kono, and T. Higuchi, *Bulletin of the Faculty of Textile Science,* Kyoto Institute of Technology, **11,** 303–350 (1987).
5. K. Sakamoto, *J. Jpn. Soc. Polym. Proc. (Seikei-Kakou),* **3,** 496–502 (1991).
6. K. Sakamoto, *Koubunshi Ronbunshuu,* **48,** 671–678 (1991).
7. C. Nonomura, T. Yamada, and T. Matsuo, *J. Jpn. Soc. Polym. Proc. (Seikei-Kakou),* **4,** 312–317 (1992).

Received February 19, 1992
Accepted June 24, 1992